ChemPubSoc Europe

DOI: 10.1002/ejoc.201801052

EurJOC European Journal of Organic Chemistry

Full Paper

SPECIAL ISSUE

Catalyst Design

Optimizing Amine-Mediated Alkyne–Allene Isomerization to Improve Benzannulation Cascades: Synergy between Theory and Experiments

Gabriel dos Passos Gomes,[a] Alec E. Morrison,[a] Gregory B. Dudley,*[b] and Igor V. Alabugin*[a]

Abstract: A synergy between theory and experiments leads to a milder protocol for base-mediated high-temperature benzannulation of alkynylpyridine substrates. Computational analysis identifies mechanistic and energetic nuances in the previously postulated 1,3-proton transfer isomerization which results in replacement of DBU with a bicyclic guanidine, 1,5,7-triazabicyclo[4.4.0]dec-5-ene (TBD). We have also outlined the general stereoelectronic and geometric hurdles for the design of 1,3-proton transfer catalysts. Considerable reductions in time, temperature, and equivalents of base underscore the potential of computational analysis to impact experimental design in the laboratory.

Introduction

Feedback loops between theory and experiment drive discovery and innovation on both fronts. Here we describe productive interplay between computational analysis and wet-lab experimentation to improve a recently developed synthesis of neopentylene-fused isoquinolines.

We recently reported the tandem cycloisomerization/elimination reaction outlined in Scheme 1 for producing substituted isoquinolines.[1] The scope of the process was reasonably broad, and the methodology produced several novel isoquinoline structures. However, there were some obvious practical drawbacks to the reported conditions. The reaction required a very high temperature, large excess of base, and extended reaction time: 210 °C, 30 equiv. 1,8-diazabicyclo[5.4.0]undec-7-ene (DBU), 2.5 days.

The base (DBU) is envisioned to play several roles in the reaction process, starting with base-catalyzed isomerization of the alkynylpyridine substrate to an allenylpyridine. The putative allenylpyridine intermediate then undergoes intramolecular inverse-demand Diels–Alder cycloaddition to provide tricycle **C**, thereby avoiding the strained cyclic allene that would arise by direct cycloaddition of alkynylpyridine **A**. Evidence for the intermediacy of **B** came in the form of deuterium incorporation at the appropriate position of neopentylene-fused isoquinoline **E** (Scheme 3). The other presumed roles of DBU are to help promote elimination of thiophenol and promote a second alkene migration (isomerization) to produce the final aromatic isoquinoline system.

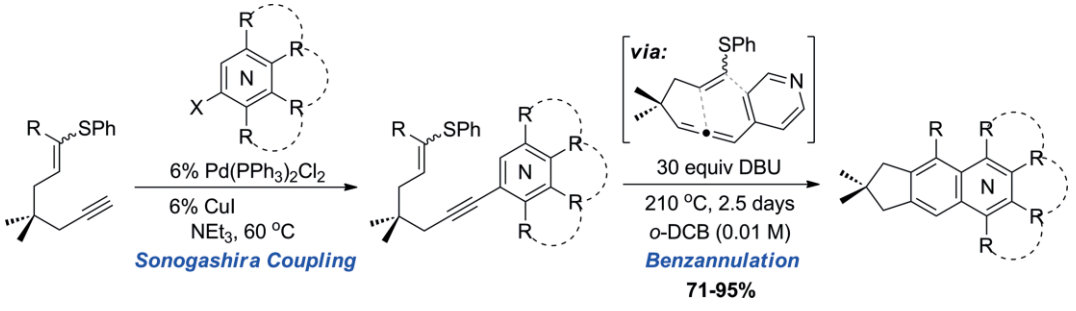

Scheme 1. Tandem isomerization/cycloaddition/elimination approach to substituted isoquinolines.

This benzannulation methodology produced a series of novel neopentylene-fused isoquinolines and related structures having unique 3D topologies and thus potentially interesting physical and pharmacological properties. Yields were generally good to excellent, and various substitution patterns were vali-

[a] Department of Chemistry and Biochemistry, Florida State University, Tallahassee, FL, 32306, USA
E-mail: alabugin@chem.fsu.edu
https://www.chem.fsu.edu/~alabugin/
[b] C. Eugene Bennett Department of Chemistry, West Virginia University, Morgantown, WV, 26505, USA
E-mail: gregory.dudley@mail.wvu.edu

Supporting information and ORCID(s) from the author(s) for this article are available on the WWW under https://doi.org/10.1002/ejoc.201801052.

dated, along with several tactics for further functionalization of substituted isoquinolines. However, as noted above, the method for producing these isoquinolines required heating to temperatures in excess for 200 °C for 2.5 days in the presence of 30 equiv. of DBU. These harsh conditions are limiting both in terms of scope and process throughput. A milder protocol would be advantageous.

Results and Discussion

We analyzed various potential reaction pathways computationally in order to guide further reaction optimization. This computational analysis of the postulated reaction pathway [(SMD = *o*-DCB)/UM06-2X/6-31+G(d,p)] provided key insights that led to identification of a milder protocol. Our analysis initially focused on the alternative cycloaddition pathways involving alkynylpyridine **A** and allenylpyridine **B** (Scheme 2). The energy diagram depicted in Scheme 2 shows comparisons between relevant species in the respective [4+2] cycloadditions of alkyne **A** to form a cyclic allene **D** (black pathway) and allenylpyridine **B** to form **C** (red pathway). At 210 °C and with the *o*-DCB solvent dielectric continuum model, the free energy of activation ($\Delta G^{\ddagger}$) for the cycloaddition involving the strained cyclic allene (**A** → **D**, black pathway) is 45.4 kcal/mol, whereas the $\Delta G^{\ddagger}$ for the allenylpyridine cycloaddition (**B** → **C**, red pathway) is only 35.5 kcal/mol. Meanwhile, allenylpyridine **B** was calculated to be 4.0 kcal/mol Lower in energy than the starting alkynylpyridine (**A**). Overall, the transition state leading to **C** was found to be 13.9 kcal/mol Lower in energy than the corresponding transition state leading to cyclic allene **D**. The path from alkynylpyridine **A** to tricycle **C** was calculated to be exergonic by 15.7 kcal/mol at 210 °C.

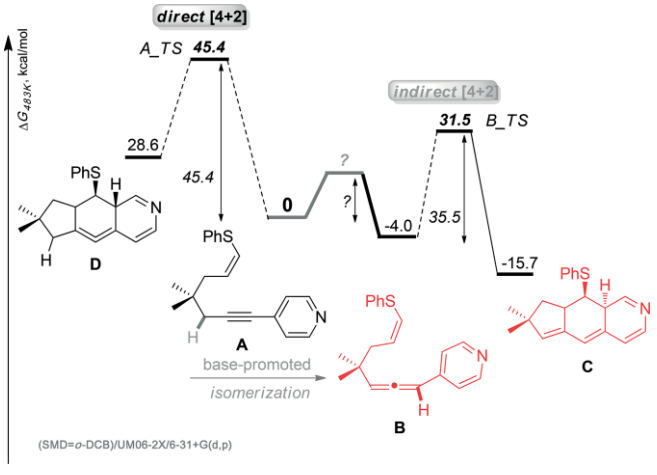

Scheme 2. Calculated free energy surfaces for the alternative cycloadditions.

Intrigued by the recently revealed evidence that cycloadditions of alkynes can proceed via non-concerted pathways,[2] we have also briefly explored the possibility of a non-concerted route via a possible diradical intermediate. However, we were not able to locate the requisite non-concerted TS. Note that most of such reports included strained reactants (e.g., *o*-benzynes), more often with more than one alkyne group.

Elimination of thiophenol and isomerization (alkene migration) to the final product (**C** → **E**) is likely initiated by deprotonation of the hydrogen illustrated in Scheme 3. Computational analysis of **C**, a truncated (didesmethyl) analogue of the starting material, revealed a hyperconjugative $\sigma_{C-H} \rightarrow \sigma^*_{C-S}$ interaction that depletes the properly aligned C–H bond from electron density as illustrated by the highest NBO charge localization in the molecule (+0.29 *e*) at the respective hydrogen atom. Furthermore, the deprotonation is assisted by gain of resonance stabilization.

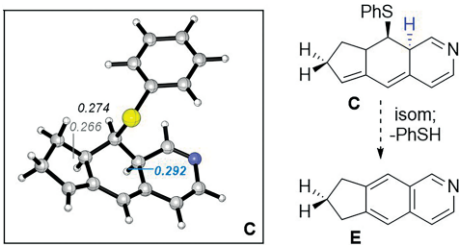

Scheme 3. Rearomatization via PhSH elimination is assisted by hyperconjugative activation of a C–H bond. Natural charges (in *e*) indicate the most positive hydrogen-atom, susceptible to deprotonation. Migration of the five-membered ring endocyclic alkene into the isoquinoline ring system occurs in parallel.

Direct cycloaddition of alkynylpyridine **A** would proceed via a highly strained (but not unprecedented)[3] cyclic allene, whereas pre-isomerization to allenylpyridine **B** enables a pathway that avoids the cyclic allene (Figure 1). This finding is another illustration of strategic advantages offered by applications of alkenes as alkyne equivalents in cascades terminated by eliminations.[4]

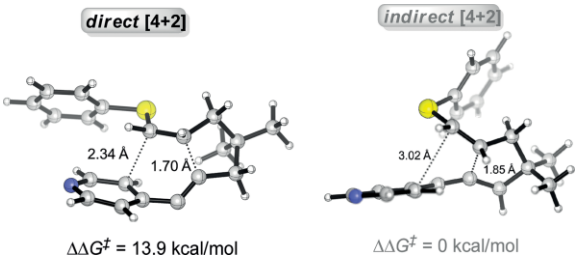

Figure 1. Transition states for the alkyne ("direct") and allene ("indirect") [4+2] cycloadditions.

Comparison of the Direct and Indirect [4+2] Transition States: the Advantage of the Indirect Route

The difference in the strain is reflected in the much more favorable thermodynamics of the indirect route (–16 vs. +29 kcal/mol). In agreement with the Hammond–Leffler postulate, the indirect TS is much earlier than the direct TS (1.85 Ang vs. 1.70 Ang).

Proton Transfer

While we observed clear energetic advantages for the putative allenylpyridine intermediate in the cycloaddition step, our computational analysis failed to reveal a clear non-catalyzed path

from alkynylpyridine **A** to allenylpyridine **B**. We were not successful in locating transition state structures or discrete intermediates corresponding to concerted or stepwise 1,3-proton transfer events. Therefore, we focused on this 1,3-proton transfer step for further experimentation and empirically driven optimization.

Considering the likely importance of the allenylpyridine intermediate and the experimentally validated need for using a large excess of DBU (30 equiv. – inferior results were obtained using 10 equiv. of DBU)[1] we elected to resume our search for alternative bases. We had previously screened lithium amides, neutral amines, metal alkoxides, and inorganic bases, and found DBU to provide the best results. Among the many unproductive bases, we initially examined were alkali metal amides of 1,3-diaminopropane, by analogy to the "alkyne zipper" reaction.[5] The zipper reagent is thought to mediate migration of an internal alkyne to a terminal position through a series of deprotonation/protonation events (formal 1,3-proton transfer), alternating between alkyne and allene *en route* to a (more acidic) terminal alkyne. The proton transfers (deprotonation and protonation) are generally represented as concerted, although discrete carbanion formation has been suggested.[6] 1,3-Proton migration reactions involving concerted and stepwise mechanisms have been discussed for other bases as well.[7] Although the alkyne zipper conditions were unsuccessful in our studies, the clearer mechanistic and energetic picture provided by computational analysis (as discussed above) refocused our attention on efforts to coordinate the presumed 1,3-proton migration. We thus explored bases that can mediate this migration in a manner analogous to the alkyne zipper reaction.

Bicyclic guanidines have received increasing attention in organocatalysis[8] for their strong Brønsted basicity and hydrogen-bonding capabilities.[9] Bicyclic frameworks can lock guanidine nitrogen atoms into orientations in which their lone pairs of electrons align with the atomic *p*-orbital of the central sp^2-hybridized carbon atom, facilitating charge delocalization in the protonated species. The favorable resonance stabilization in the positively charged species is associated with increased basicity for bicyclic guanidine bases compared to amidine bases like DBU, which feature one fewer nitrogen-centered lone pair of electrons (Scheme 4).[10] There are several examples of guanidine bases synthetically outperforming their amidine counterparts,[11] and we have an ongoing interest in the utility of guanidines as polyfunctional nucleophiles.[12]

The increased basicity coupled with a conveniently located exchangeable proton led us to explore bicyclic guanidines in our isoquinoline synthesis. We envisioned that the 1,3-proton transfer could take place in a concerted or rapid stepwise manner by analogy to 1,3-proton transfers mediated by metallated 1,3-diaminopropane (Scheme 4).

Replacing DBU with the bicyclic guanidine 1,5,7-triazabicyclo[4.4.0]dec-5-ene (TBD) resulted in a comparable yield for the conversion of alkynylpyridine **A** to isoquinoline **E** (78 % vs. 81 %) but with considerable reduction in time (24 h vs. 2.5 d), temperature (180 °C vs. 210 °C), and equivalents of base (2 equiv. vs. 30 equiv.). Substoichiometric quantities of TBD failed to produce full conversion, suggesting that the thiophenol produced during the course of the reaction may stoichiometrically attenuate the basicity of the TBD (Scheme 5).

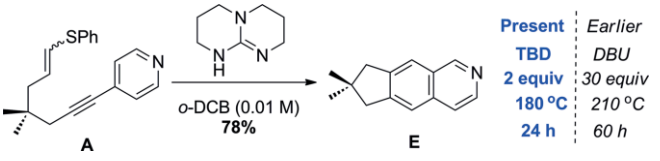

Scheme 5. Improved cascade efficiency in the presence of TBD.

We could not locate a concerted path for the TBD-mediated 1,3-proton transfer. However, a stepwise path was identified using guanidine itself and a simplified alkynylpyridine. Abstraction of the propargylic proton by guanidine proceeds via a transition state that is higher in energy than the separated reactants by ≈ 36 kcal/mol (Scheme 6).[13] Although this number is high, it is still considerably lower than the 45 kcal/mol barrier for the direct [4+2] cyclization of the alkyne **A**. Although the charge-separated structure that results from the proton transfer (the guanidinium salt of propargylic carbanion) corresponds to a local minimum at the enthalpic surface, it is located even higher than the TS at the free energy surface due to the entropic penalty.

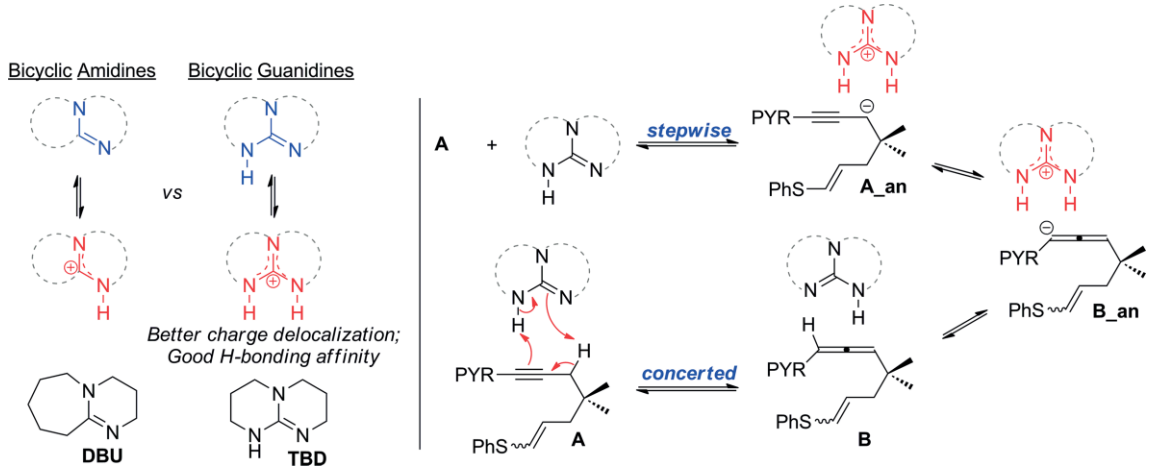

Scheme 4. Mechanistic hypothesis and design for the prototropic alkyne/allene isomerization.

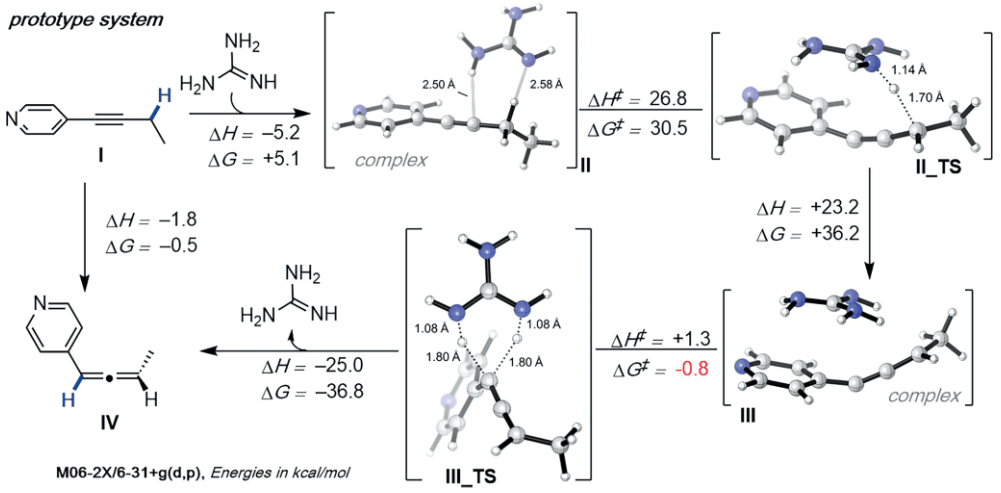

Scheme 6. Calculated PES for a guanidine-mediated alkyne–allene isomerization.

The allene-forming proton transfer to the carbanion from guanidinium is likely to be very fast, still providing a path that is energetically preferable to the direct [4+2] addition. Our attempts to locate such a TS lead to a TS that corresponds to proton shuffling at the benzylic position of allene by guanidinium. The proton delivery from guanidinium ion to carbanion may (but does not have to) proceed through the same transition state. Such a process would correspond to a bifurcation[14] that connects the charge separated carbanion/guanidinium pair to both stereoisomers of the allene intermediate. From this analysis, it is clear that the alkyne/allene isomerization via the formal 1,3-proton transfer is an interesting mechanistic challenge for the future studies.

TBD-catalyzed alkyne–allene isomerization is also asynchronous (Scheme 7). Although the free energy barrier is lower than guanidine (from ≈ 36 to ≈ 28 kcal/mol), the 2nd proton transfer lags behind.

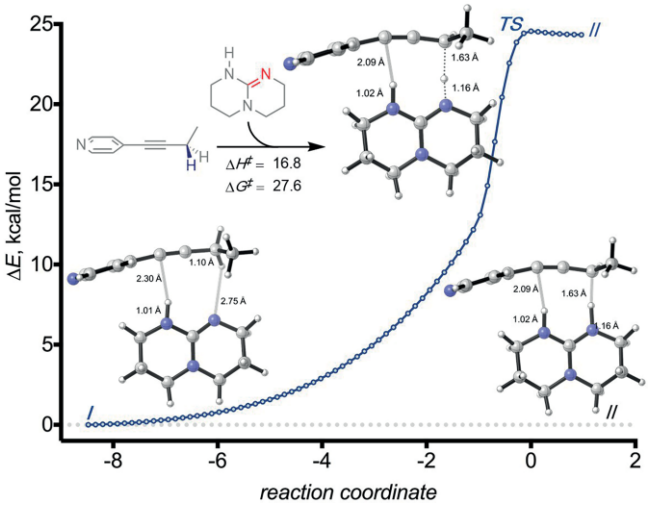

Scheme 7. TBD-catalyzed alkyne–allene isomerization.

Comparison of the substrate/base pre-reaction complex and the TS reveals the stereoelectronic dichotomy of guanidine and illustrates why the proton shift remained difficult with guanidine-based catalysts (Scheme 8, top). In the pre-reaction complex, the lone pair of the imine moiety hydrogen-bonds with the propargylic C–H. This orientation allows one of the N–H bonds to coordinate with one of the alkyne carbons in a geometry that would be suitable for the concerted 1,3-proton transposition. However, the imine lone pair is a relatively poor donor due to the low orbital energy associated with the large amount of s-character.[15] Furthermore, the concerted process would require breaking a C–H bond simultaneously with breaking the N–H bond of the NH_2 group. Unlike the stereoelectronically weakened propargylic C–H bond, the N–H bond at the sp^2 nitrogen atom of the NH_2 group is orthogonal to the guanidine pi-system. Hence, breaking of this strong N–H bond is not assisted by stereoelectronics.

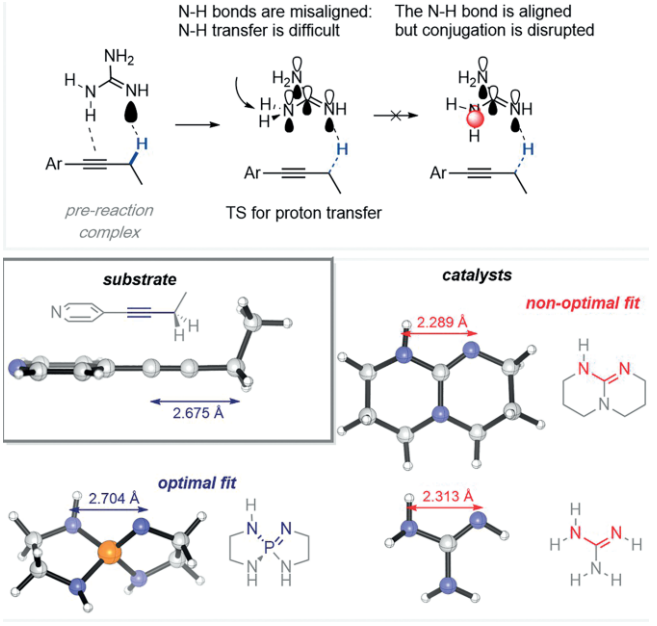

Scheme 8. Top: Stereoelectronic frustration in the design of 1,3-proton transfer processes. Bottom: Geometric mismatch for 1,3-proton transfer in propargylic systems and its possible solution.

A better route to utilizing the donor ability of the guanidine bases is to use the delocalized pi-system where the donor ability of the C=N π-bond is enhanced by *p*-type lone pairs of the two NH_2 groups.[16] The HOMO of guanidine is a π-type orbital that includes these lone pairs. Hence, in the TS for propargylic proton abstraction, the guanidine molecule could have benefited from reorienting itself ≈ 90 degrees relative to the geometry of the pre-reaction complex, so the relatively strong basicity of the catalyst would assist in the propargylic C–H deprotonation. However, the 90-degree reorientation makes concerted N–H transfer to the anion geometrically difficult. Rotation of one of the NH_2 groups that would fix the geometric problem should be highly unfavorable energetically because it has to disrupt conjugation in the guanidinium moiety. These observations help rationalize why a concerted guanidine-catalyzed alkyne/allene isomerization is difficult.

Furthermore, there is an additional geometric problem (Scheme 8, bottom). When three atoms are positioned in a linear (or near-linear) geometry enforced by sp-hybridization of the alkyne, the distance between them has to be greater than the distance between three atoms at a bent geometry of the NCN moiety of the catalyst. The difference in distances is quite significant (≈ 2.7 Å vs. 2.3 Å).

The geometric mismatch can be fixed by using a larger central atom X in the N=X–N triade. Inspired by a suggestion from one the referees for this manuscript, we have evaluated the possibility of concerted proton transfer using a phosphorus-based catalyst where the longer P–N bonds make the distance between the acidic (N–H) and the basic (N) centers of the catalyst to match closely the 1,3-carbon distance in the propargylic reagent (2.70 Å vs. 2.68 Å). Indeed, the catalyst can promote the 1,3-proton shift in propyne via a ≈ 3 kcal/mol Lower (27 kcal/mol) TS (Scheme 9).[17]

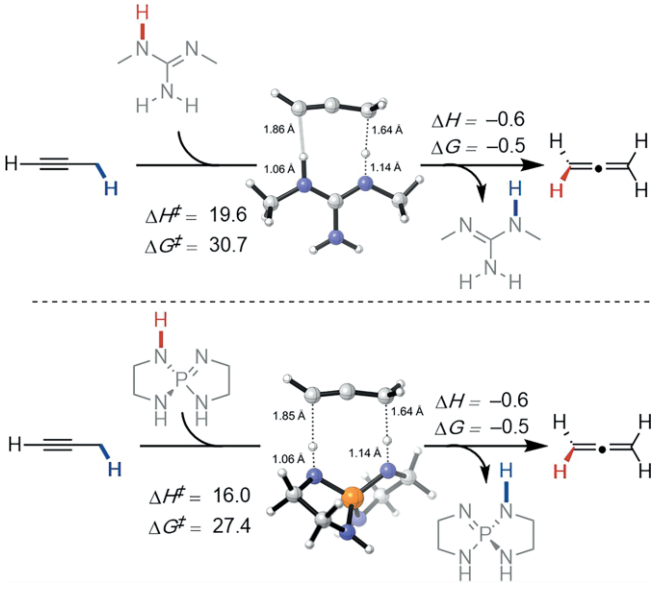

Scheme 9. Comparison of *N*,*N*′-dimethylguanidine- and NPN-catalyzed alkyne–allene isomerization in the parent propyne/1,2-propadiene system. Activation and reaction energies are given relative to the isolated reactants.

Nevertheless, even for the P-containing catalyst the pattern and the extent of proton transfer remained similar to *N*,*N*′-dimethylguanidine-catalyzed process. Importantly, the process remained distinctly asynchronous, with the 2nd proton transfer lagging noticeably behind the 1st proton transfer (Scheme 10).

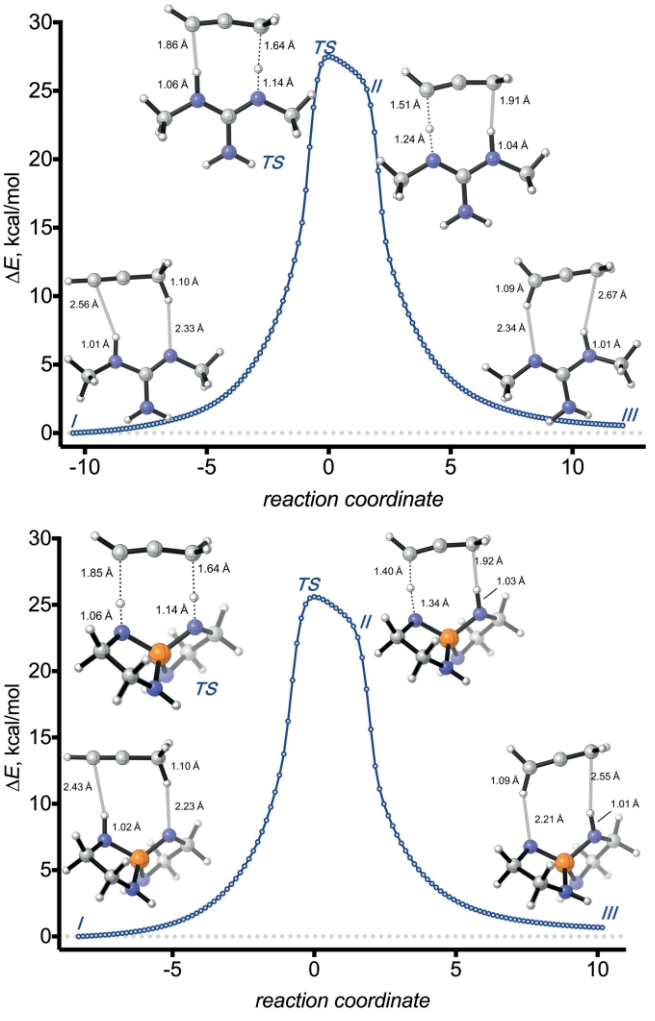

Scheme 10. Intrinsic reaction coordinate (IRC) scans for *N*,*N*′-dimethylguanidine-(top) and NPN-catalyzed (bottom) alkyne–allene isomerization in the parent propyne/1,2-propadiene system reveal hidden transition states corresponding to the second proton transfer step (geometry II) in the "barrierless" transition from the main TS to the product.

We have also evaluated the possibility of accelerating the proton shift by taking a catalyst where both the acid and base centers are activated relative to the parent *N*,*N*′-dimethylguanidine. Such modification can be accomplished without geometric perturbations by using a proton tautomer of *N*,*N*′-dimethylguanidine as the catalyst. Scheme 11 illustrates the efficiency of this approach by presenting the IRC for alkyne/allene isomerization catalyzed by this zwitterionic molecule.

In this highly exothermic reaction, the driving force (ΔE_{rxn} ≈ –30 kcal/mol), comes mostly from converting charge-separated catalyst to its more stable guanidine tautomer. It is important to point out the highly asynchronous nature of the process. In the electronic PES, the first proton transfer occurs from the propargylic position to the base (Scheme 11, TS). This point corresponds to the overall TS for the reaction: analysis of its frequencies reveals a strong vibration corresponding to the ex-

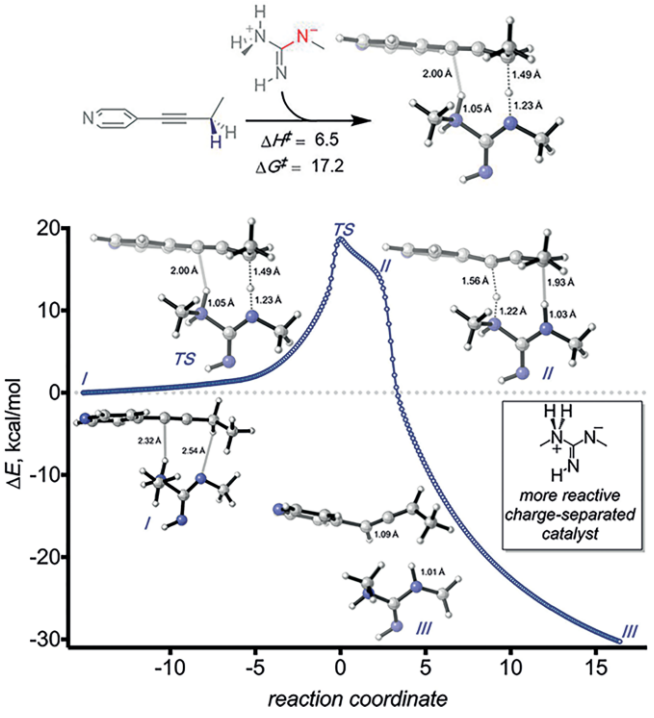

Scheme 11. IRC for alkyne/allene isomerization with a proton tautomer of dimethylated guanidine shows the lack of synchronicity for 1,3-proton transfer.

pected proton motion, coupled with a weak vibration for the proton that will be transferred later. Point II corresponds to the second proton transfer from the catalyst to the negatively charged allene moiety. This shoulder indicates that the driving force to avoid charge separation lowers the potential second TS energy so much that the reaction proceeds without an intermediate,[18] albeit in a highly asynchronous manner. Understanding of the dynamics controlling these types of reactions is key to the design of better catalysts.[19]

Conclusions

In conclusion, computational analysis of a base-mediated high-temperature benzannulation supports the previously postulated allenylpyridine intermediates, which can arise by base-mediated stepwise 1,3-proton transfer isomerization of the alkynylpyridine substrates. Allenylpyridine **B** was calculated to be 4.0 kcal/mol Lower in energy than alkynylpyridine **A**, and the transition state energy associated with cycloisomerization was calculated to be 13.9 kcal/mol Lower in energy for allenylpyridine **B** than for alkynylpyridine **A**. We were unable to locate a reasonable transition state or intermediate for the DBU-mediate isomerization of **A** → **B**, which prompted us to focus on this postulated mechanistic step for further optimization of the protocol. Switching the base from DBU to TBD enabled the benzannulation reaction to proceed more rapidly and under milder conditions, which we expect will be associated with a broader scope and enhanced synthetic utility of the method. However, even under the TBD-mediated conditions, the alkyne/allene isomerization remained difficult.

We have identified stereoelectronic difficulties for engineering a truly concerted 1,3-proton transfer in alkyne/allene isomerization. Two possible design strategies offer themselves for the development of more efficient versions of the catalysts – a) the use of longer P–N bonds to fix the geometric mismatch between the substrate and the catalyst or b) the increase the electronic assistance to the deprotonation/reprotonation sequence by making the basic and acidic centers in the catalyst more reactive. Expansion of this methodology to include the synthesis of other polycyclic aromatic systems is planned.

Experimental Section

Representative Experimental Procedure: To a 1,2-dichlorobenzene solution (0.01*M*) of phenylthioenyne **A** (*E*/*Z* = 2.5:1, 0.10 g, 0.33 mmol, 1 equiv.) in a sealed tube was added 1,5,7-triazabicyclo[4.4.0]dec-5-ene (0.09 g, 0.65 mmol, 2 equiv.). Once sealed, the mixture was heated to 180 °C for 24 h. After 24 h, the reaction mixture was cooled to room temperature before being directly loaded onto a silica gel column without removal of solvent and further eluted with gradient eluent from EtOAc/hexane = 1:99 to EtOAc/hexane = 10:90 to give **E** (0.05 g, 78 % yield) as a yellow solid. Spectroscopic data were identical to the reported data from the literature.[1]

Computational Details: To gain deeper insight into the origin of observed selectivities, we have evaluated the relative thermodynamic stabilities using the *meta*-hybrid M06-2X functional. The M06-2X functional has demonstrated good thermodynamic trends for organic reactions. For more details, see.[20] We used solvation corrections when necessary (SMD[21] = *o*-DCB). We employed Natural Bond Orbital (NBO)[22] analysis for quantifying stereoelectronic interactions and atomic charges. The 6-31+G(d,p) basis set was employed for all systems. Frequency calculations were carried for all structures to confirm them as either a minimum or a TS. Intrinsic reaction coordinates (IRC)[23] were determined for the TS of interest. *Gaussian '09* was used for all calculations. Molecular geometries were rendered with CYLView 1.0.1.[24] A dataset collection of all computational results (including geometries and energies) can be found in the ioChem-DB repository,[25] where it can be accessed at https://iochem-bd.bsc.es/browse/handle/100/192812.

Acknowledgments

We thank the National Science Foundation for support of this research: CHE-1300722 (G. B. D. and I. V. A.), CHE-1834949 (G. B. D.), and CHE-1800329 (I. V. A.). We also appreciate a helpful suggestion of one of the reviewers regarding the use of phosphorus-containing proton-transfer catalysts.

Keywords: Benzannulation · Alkynes · Allenes · Proton transfer · Isomerization · Guanidines

[1] A. E. Morrison, J. J. Hrudka, G. B. Dudley, *Org. Lett.* **2016**, *18*, 4104–4107.
[2] a) Ref. 3l; b) Y. Wang, T. R. Hoye, *Org. Lett.* **2018**, *20*, 4425–4429; c) X. Xiao, B. P. Woods, W. Xiu, T. R. Hoye, *Angew. Chem. Int. Ed.* **2018**, *57*, 9901–9905; *Angew. Chem.* **2018**, *130*, 10049–10053; d) M. Stiles, U. Burckhardt, *J. Am. Chem. Soc.* **1964**, *86*, 3396; e) S. Umezu, G. P. Gomes, T. Yoshinaga, M. Sakae, K. Matsumoto, T. Iwata, I. V. Alabugin, M. Shindo, *Angew. Chem. Int. Ed.* **2016**, *55*, 1–6; *Angew. Chem.* **2016**, *128*, 1–6.

[3] a) P. Wessig, G. Müller, *Chem. Rev.* **2008**, *108*, 2051–2063; b) D. Rodríguez, A. Navarro-Vázquez, L. Castedo, D. Domínguez, C. Saá, *J. Org. Chem.* **2003**, *68*, 1938–1946; c) D. Rodríguez, A. Navarro-Vázquez, L. Castedo, D. Domínguez, C. Saá, *J. Am. Chem. Soc.* **2001**, *123*, 9178–9179; d) R. C. Burrell, K. J. Daoust, A. Z. Bradley, K. J. DiRico, R. P. Johnson, *J. Am. Chem. Soc.* **1996**, *118*, 4218; e) A. Z. Bradley, R. P. Johnson, *J. Am. Chem. Soc.* **1997**, *119*, 9917–9918; f) T. R. Hoye, B. Baire, D. Niu, P. H. Willoughby, B. P. Woods, *Nature* **2012**, *490*, 208–212; g) V. Palani, J. Chen, T. R. Hoye, *Org. Lett.* **2016**, *18*, 6312–6315; h) T. Wang, T. R. Hoye, *J. Am. Chem. Soc.* **2016**, *138*, 13870–13873; i) F. Xu, K. W. Hershey, R. J. Holmes, T. R. Hoye, *J. Am. Chem. Soc.* **2016**, *138*, 12739–12742; j) F. Xu, X. Xiao, T. R. Hoye, *Org. Lett.* **2016**, *18*, 5636–5639; k) J. Zhang, D. Niu, V. A. Brinker, T. R. Hoye, *Org. Lett.* **2016**, *18*, 5596–5599; l) T. Wang, D. Niu, T. R. Hoye, *J. Am. Chem. Soc.* **2016**, *138*, 7832–7835; m) F. Xu, X. Xiao, T. R. Hoye, *J. Am. Chem. Soc.* **2017**, *139*, 8400–8403.

[4] a) G. P. Gomes, C. Evoniuk, M. Ly, I. V. Alabugin, *Org. Biomol. Chem.* **2017**, *15*, 4135–4143; b) C. Evoniuk, G. P. Gomes, M. Ly, F. White, I. V. Alabugin, *J. Org. Chem.* **2017**, *82*, 4265–4278; c) R. K. Mohamed, S. Mondal, J. V. Guerrera, T. M. Eaton, T. E. Albrecht-Schmitt, M. Shatruk, I. V. Alabugin, *Angew. Chem. Int. Ed.* **2016**, *55*, 12054–12058; *Angew. Chem.* **2016**, *128*, 12233–12237; d) R. K. Mohamed, S. Mondal, K. Jorner, T. Faria Delgado, H. Ottosson, I. V. Alabugin, *J. Am. Chem. Soc.* **2015**, *137*, 15441–15450; e) C. J. Evoniuk, M. Ly, I. V. Alabugin, *Chem. Commun.* **2015**, *51*, 12831–12834; f) R. Mohamed, S. Mondal, B. Gold, C. J. Evoniuk, T. Banerjee, K. Hanson, I. V. Alabugin, *J. Am. Chem. Soc.* **2015**, *137*, 6335–6349; g) S. Mondal, B. Gold, R. K. Mohamed, I. V. Alabugin, *Chem. Eur. J.* **2014**, *20*, 8664–8669.

[5] C. A. Brown, A. Yamashita, *J. Am. Chem. Soc.* **1975**, *97*, 891–892.

[6] S. R. Abrams, A. C. Shaw, *J. Org. Chem.* **1987**, *52*, 1835–1839.

[7] a) D. J. Cram, F. Willey, H. P. Fischer, H. M. Relles, D. A. Scott, *J. Am. Chem. Soc.* **1966**, *88*, 2759–2766; b) J. H. Wotiz, P. M. Barelski, D. F. Koster, *J. Org. Chem.* **1973**, *38*, 489–493; c) R. J. Bushby, G. H. Whitham, *J. Chem. Soc. B* **1969**, 67; d) V. B. Kobychev, N. M. Vitkovskaya, N. S. Klyba, B. A. Trofimov, *Russ. Chem. Bull.* **2002**, *51*, 774–782.

[8] a) H. Liu, D. Leow, K.-W. Huang, C.-H. Tan, *J. Am. Chem. Soc.* **2009**, *131*, 7212; b) M. K. Kiesewetter, M. D. Scholten, N. Kirn, R. L. Weber, J. L. Hedrick, R. M. Waymouth, *J. Org. Chem.* **2009**, *74*, 9490; c) H. Xue, D. Jiang, H. Jiang, C. W. Kee, H. Hirao, T. Nishimura, M. W. Wong, C.-H. Tan, *J. Org. Chem.* **2015**, *80*, 5745.

[9] M. P. Coles, *Chem. Commun.* **2009**, 3659–3676.

[10] I. Kaljurand, A. Kütt, L. Sooväli, T. Rodima, V. Mäemets, I. Leito, I. A. Koppel, *J. Org. Chem.* **2005**, *70*, 1019–1028.

[11] a) N. H. Park, G. P. Gomes, M. Fevre, G. O. Jones, I. V. Alabugin, J. L. Hedrick, *Nat. Commun.* **2017**, *8*, 166; b) S. Martinez-Erro, A. SanzMarco, A. B. Gomez, A. Vazquez-Romero, M. S. G. Ahlquist, B. Martin-Matute, *J. Am. Chem. Soc.* **2016**, *138*, 13408–13414.

[12] a) S. F. Vasilevsky, D. S. Baranov, V. I. Mamatyuk, D. S. Fadeev, Y. V. Gatilov, A. A. Stepanov, N. V. Vasilieva, I. V. Alabugin, *J. Org. Chem.* **2015**, *80*, 1618–1631; b) S. F. Vasilevsky, D. S. Baranov, V. I. Mamatyuk, Y. V. Gatilov, I. V. Alabugin, *J. Org. Chem.* **2009**, *74*, 6143–6150.

[13] Note that this reaction is significantly less favourable that proton transfer from the much more acidic propargylic carbons additionally activated by electron-accepting groups: a) D. Huang, S. Qin, C. Hu, *Org. Biomol. Chem.* **2011**, *9*, 6034; b) H. Xiao, Y. Kobayashi, Y. Takemoto, K. Morokuma, *ACS Catal.* **2016**, *6*, 2988.

[14] a) B. K. Carpenter, *J. Am. Chem. Soc.* **1985**, *107*, 5730–5732; b) S. L. Debbert, B. K. Carpenter, D. A. Hrovat, W. T. Borden, *J. Am. Chem. Soc.* **2002**, *124*, 7896–7897; c) B. K. Carpenter, J. N. Harvey, A. J. Orr-Ewing, *J. Am. Chem. Soc.* **2016**, *138*, 4695–4705; d) C. Doubleday Jr., K. Bolton, W. L. Hase, *J. Am. Chem. Soc.* **1997**, *119*, 5251–5252; e) C. Doubleday, C. P. Suhrada, K. N. Houk, *J. Am. Chem. Soc.* **2006**, *128*, 90–94; f) Z. Chen, Y. Nieves-Quinones, J. R. Waas, D. A. Singleton, *J. Am. Chem. Soc.* **2014**, *136*, 1312–1319; g) Y. Nieves-Quinones, D. A. Singleton, *J. Am. Chem. Soc.* **2016**, *138*, 15167–15176; h) D. J. Tantillo, *J. Am. Chem. Soc.* **2014**, *136*, 2450–2463; i) B. Biswas, D. A. Singleton, *J. Am. Chem. Soc.* **2015**, *137*, 14244–14247; j) K. N. Sedenkova, E. B. Averina, Y. K. Grishin, J. V. Kolodyazhnaya, V. B. Rybakov, T. S. Kuznetsova, A. Hughes, G. D. P. Gomes, I. V. Alabugin, N. S. Zefirov, *Org. Biomol. Chem.* **2017**, *15*, 9433–9441.

[15] I. V. Alabugin, S. Bresch, G. P. Gomes, *J. Phys. Org. Chem.* **2015**, *28*, 147–162.

[16] I. V. Alabugin, *Stereoelectronic Effects: The Bridge between Structure and Reactivity*. John Wiley & Sons Ltd, Chichester, UK, **2016**.

[17] We are grateful to an anonymous reviewer for providing this transition state geometry.

[18] For analysis of electronic effects that lead to "hidden transition states", see D. V. Vidhani, J. W. Cran, M. E. Krafft, M. Manoharan, I. V. Alabugin, *J. Org. Chem.* **2013**, *78*, 2059–2073; D. Vidhani, M. Krafft, I. V. Alabugin, *J. Am. Chem. Soc.* **2016**, *138*, 2769–2779.

[19] Note that a similar PES shape is observed for the two tautomerizations described with the two bifunctional catalysts in Scheme 10.

[20] The M06-2X functional has demonstrated to provide good thermodynamic data for organic reactions. For more details, see: a) Y. Zhao, D. G. Truhlar, *Theor. Chem. Acc.* **2008**, *120*, 215; b) Y. Zhao, D. G. Truhlar, *Acc. Chem. Res.* **2008**, *41*, 157.

[21] A. V. Marenich, C. J. Cramer, D. G. Truhlar, *J. Phys. Chem. B* **2009**, *113*, 6378.

[22] a) F. Weinhold, C. R. Landis, E. D. Glendening, *Int. Rev. Phys. Chem.* **2016**, *35*, 1; A. E. Reed, F. J. Weinhold, *Chem. Phys.* **1985**, *83*, 1736; b) A. E. Reed, F. Weinhold, *Isr. J. Chem.* **1991**, *31*, 277; c) A. E. Reed, L. A. Curtiss, F. Weinhold, *Chem. Rev.* **1988**, *88*, 899; d) F. Weinhold, Schleyer P. v. R. *Encyclopedia of Computational Chemistry*, Wiley, New York, **1998**, pp. 3, 1792.

[23] K. Fukui, *Acc. Chem. Res.* **1981**, *14*, 363.

[24] *CYLview*, 1.0b; C. Y. Legault, Université de Sherbrooke, **2009** (http://www.cylview.org).

[25] https://iochem-bd.bsc.es/. For the explanatory paper, please see: M. Álvarez-Moreno, C. de Graaf, N. López, F. Maseras, J. M. Poblet, and C. Bo, *J. Chem. Inf. Model.* **2015**, *55*, 95–103.

Received: July 5 2018

